

A Friendly Approach to Increasing the Frequency Response of Piezoelectric Generators

Sam Ben-Yaakov, Gil Hadar, Amit Shainkopf and Natan Krihely

Power Electronics Laboratory,
Department of Electrical and Computer Engineering
Ben-Gurion University of the Negev,
P.O.Box 653, Beer-Sheva 84105, ISRAEL

Abstract— A wide bandwidth piezoelectric generator (PZG) was constructed and tested experimentally. The PZG was characterized using chirp and wideband random excitations. The experimental results showed that by proper shaping of an attached cantilever beam it is possible to increase the number of vibration modes of the PZG and, hence, to improve the effectiveness of the energy harvesting as compared with a conventional cantilever PZG configuration. The proposed structure was designed to produce 3 vibration modes, which extend the operation around the frequencies 35Hz, 57Hz and 76Hz. As a result, the bandwidth was widened by a factor of 2.81 as compared with a conventional harvester.

Keywords—Harvesting, piezoelectric devices, resonant power conversion.

I. INTRODUCTION

Ambient mechanical vibration energy is characterized by different frequency spectra. A piezoelectric harvester is a high Q resonant device that can effectively pick up ambient vibration energy only at or near a particular resonant frequency. This is also evident from the expression of the output average power P_{avg} as function of vibration frequency [1],

$$P_{avg} = \frac{m\zeta\delta^2(f/f_{res})^3}{[1-(f/f_{res})^2]^2 + (2\zeta f/f_{res})^2} \quad (1)$$

where f_{res} is the resonant frequency and m , ζ and δ are parameters of the PZG. In applications where the frequency of ambient vibration varies periodically, such as in vehicles and with human motion, the PZG might not always be tuned to the resonance condition. As a result, the efficiency of a PZG with one fixed resonant mode at frequency f_{res} drops significantly (1).

Increasingly, efforts are being made to develop broadband energy harvesters that can harvest energy over a large frequency interval. Typically, this is achieved by electrically and/or mechanically connecting energy harvesters whose operating frequencies are slightly different from, but very close to each other [2]. However, these assembled generators must be carefully designed so that each individual generator does not effect the others. This makes such a configuration more complex to design and fabricate and the final volume of the device depends on the number of PZGs utilized. It has also

been shown that bandwidth widening can be achieved using mechanical stoppers, nonlinear springs or bi-stable structures [3]-[5]. These strategies can be broadly classified as: 1) bandwidth widening along with increased output power, 2) bandwidth widening without power enhancement.

A conventional PZG harvester usually consists of piezoelectric cantilever beam (Fig. 1a) with or without a proof mass attached to the free end. The other end of the harvester is bonded to a vibrating base. All commercial PZGs exhibit this elementary configuration [6]. However, a limitation of this approach lies in the fact that the generator is, by definition, designed to work at a single frequency (1).

This study demonstrates a simple and friendly solution to extend the frequency response of the generator, based on the work presented in [7]. The behavior of energy harvesting systems subject to a random broadband excitation is less obvious than the classic sinusoidal case [8]. Therefore, the efficacy of the proposed configuration has been demonstrated under the effect of abnormal vibrations.

II. PROPOSED STRUCTURE

In many piezoelectric harvesting applications, a conventional PZG includes one or more piezoelectric transducer (PZT) patches that are attached to a flexible beam [9]. Such a concept underpins the conventional cantilever-based generator shown in Fig. 1a. As can be seen in the figure, an additional beam has been clamped to the PZG using a clamping support and screws. In our work, this rectangular beam-based harvester serves as a reference structure, denoted henceforth as “conventional PZG”. A commercial piezoelectric bimorph V20W (Mide Technology) [6] has been selected as the basic platform to be improved.

The proposed PZG depicted in Fig. 1b is targeted to the following key objectives [7]:

- 1) simplified configuration construction approach,
- 2) cost- and volume- effectiveness,
- 3) matching practical ambient vibration frequencies around 30Hz-200Hz [1].

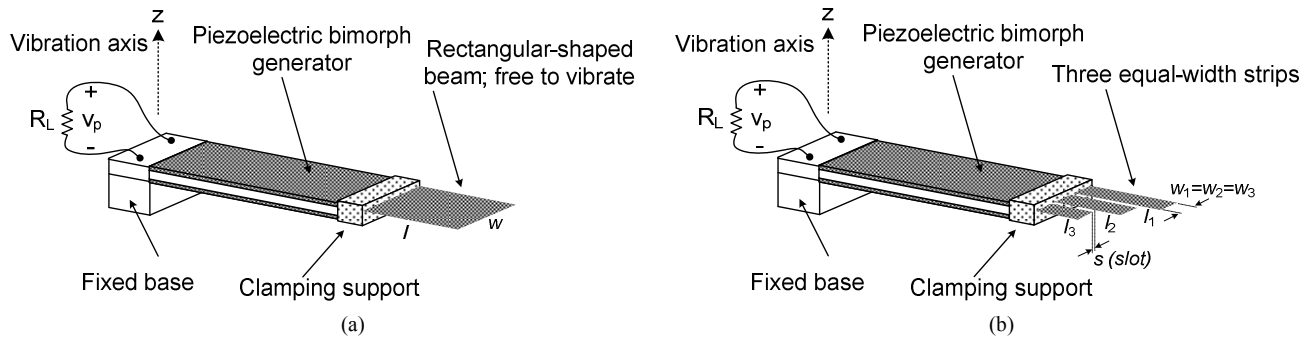


Fig. 1. Schematic of the piezoelectric generator with a cantilever beam: (a) rectangular beam, (b) proposed beam with three equal-width fingers.

TABLE I
STRUCTURAL PARAMETERS OF BOTH STRUCTURES

Conventional PZG		Proposed PZG	
Parameter	Value	Parameter	Value
Beam width	$w=43\text{mm}$	Finger width	$w_1=w_2=w_3=13.5\text{mm}$
Beam length	$l=30\text{mm}$	1 st finger length	$l_1=44\text{mm}$
-		2 nd finger length	$l_2=30\text{mm}$
-		3 rd finger length	$l_3=21\text{mm}$
-		Slot	$s=0.8\text{mm}$
Beam area	$l \cdot w=1290\text{mm}^2$	Beam area	$l_1 \cdot w_1 + l_2 \cdot w_2 + l_3 \cdot w_3=1282\text{mm}^2$
Material	Brass	Material	Brass
Thickness	0.1mm	Thickness	0.1mm

It should be noted that the surface of the extra beam that extends beyond the bonded area of either structure was not covered by any PZT layers or patches. It is known that adding additional mass or, alternatively, extending the supporting beam, alters the frequency response of the system [10]. This causes a decrease in the working frequency, which is usually preferred for many practical applications with low-frequency ambient vibrations [1].

Subject to the volume criteria (objective 2, above), the dimensions of the attached beam were constrained to the dimensions of the hosting platform. The attached beam of the proposed configuration (Fig. 1b) has been shaped to include an array composed of three fingers of different lengths, l_1 , l_2 , l_3 , but with the same width, $w_1=w_2=w_3$. The parameters l_1 , l_2 , l_3 describe the lengths extending out beyond the clamping support. A residual section of the beam penetrates between the clamping support and the given platform. Thereby, the three parts overlap for 10mm along the beam. A very small gap, or slot, s , has been introduced between the fingers to allow free movement. Apart from shifting down the fundamental resonant frequency of the original structure, the aim of this concept is to create new vibration modes due to the individual mechanical responses of each finger strip. The geometrical properties of the proposed configuration are summarized in Table I. In both structures, the two attached beams had approximately the same total surface area of 1290mm^2 and the same material thickness.

III. PERFORMANCE EVALUATION

In this section we investigate the performance of the proposed PZG. In the experimental setup, the energy harvesting systems were excited vertically by a LING

laboratory shaker with a bandwidth of 9KHz (model V406). The input base acceleration level was monitored using an Analog Devices ADXL327 accelerometer with sensitivity and bandwidth of 462mV/g and 1.6KHz, respectively.

In the following study we conducted a comparison between the two considered configurations (Fig. 1) in terms of the frequency response and the average output power under chirp and random excitations.

A. Chirp excitation

The dominant flexural modes of each prototype were first determined by applying a chirp excitation signal over the frequency range 1-200Hz with a period of 10sec and by measuring the open circuit voltage output with respect to the $1\text{M}\Omega$ input resistance of the oscilloscope. The amplitude of the acceleration was maintained at a fixed level of 0.45g. The time domain output voltage, v_p , of both structures was recorded (Fig. 2). It is evident from Fig. 2 that when the input frequency approaches a certain vibration mode (resonant frequency), the voltage increases significantly and then drops as the input frequency changes. Fig. 2a reveals that the prototype with a rectangular beam yields one dominant frequency at 58Hz. On the other hand, the configuration with the three finger beams produced locally maximal open circuit voltages at 35Hz, 57Hz and 76Hz (Fig. 2b). Hence, two additional dominant vibration modes were created as a result of splitting the beam into 3 different length fingers. This comprises the widening effect of the frequency response, which can be further controlled by adjusting the properties of the beam (length, shape, proportion etc.).

Let us define a local bandwidth as the frequency range from the first -3dBV occurrence up to the second one for each frequency mode. The bandwidth of the rectangular beam cantilever is found to be $\Delta f_{\text{res}}=4.4\text{Hz}$. Fig. 2b of the proposed structure reveals bandwidths of $\Delta f_1=3.8\text{Hz}$, $\Delta f_2=4.1\text{Hz}$, $\Delta f_3=4.5\text{Hz}$.

$$\frac{\Delta f_{r1} + \Delta f_{r2} + \Delta f_{r3}}{\Delta f_{res}} \approx 2.81 \quad (2)$$

Hence, (2) implies a bandwidth widening factor of 2.81 compared to the conventional case.

In addition, the input capacitance, C_p , of the PZG platform was measured to be 34.5nF by an LCR meter working at an operating frequency of 1KHz, (well above the dominant modes of the structures). It should be noted that the internal capacitance, C_p , is common to both structures because the attached beams are free of any PZT material.

B. Random excitation

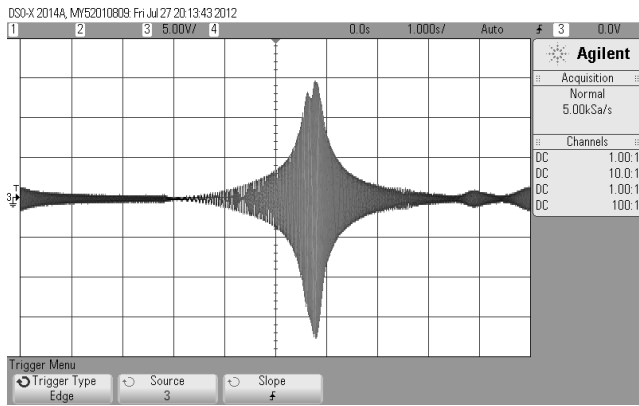
Most previously reported research has focused on an idealized single sinusoidal input, which is valuable for

section, the useful frequency range of the two configurations was identified to exist around the 100Hz frequency band. The random driving force was generated by an Agilent 33220A arbitrary waveform generator. The generated signal was constructed with a time period of 10sec and a sampling frequency of 6.4KHz.

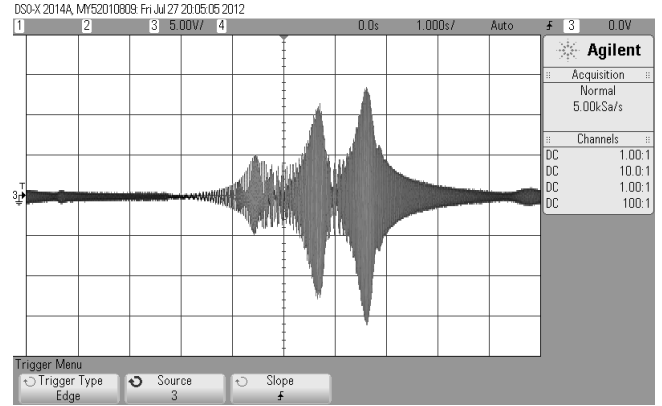
The average powers are derived from the steady-state time response in a 50sec interval (Fig. 3),

$$P_L = \frac{V_{p(rms)}^2}{R_L} = \frac{1}{R_L} \int_0^{50} v_p^2 dt \quad (3)$$

where P_L , v_p , R_L and $V_{p(rms)}$ are, respectively, the average output power, the instantaneous output voltage of the generator, the output load and the rms value of v_p .

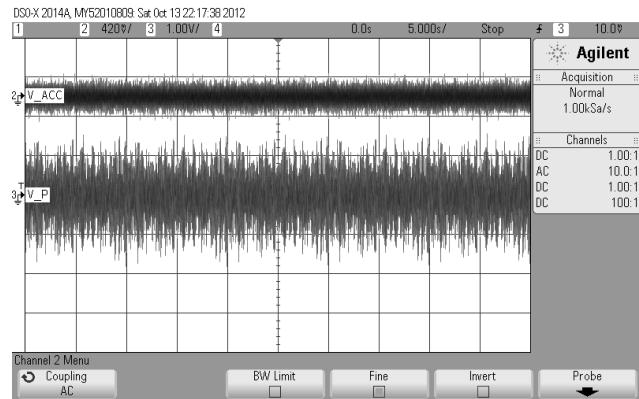


(a)

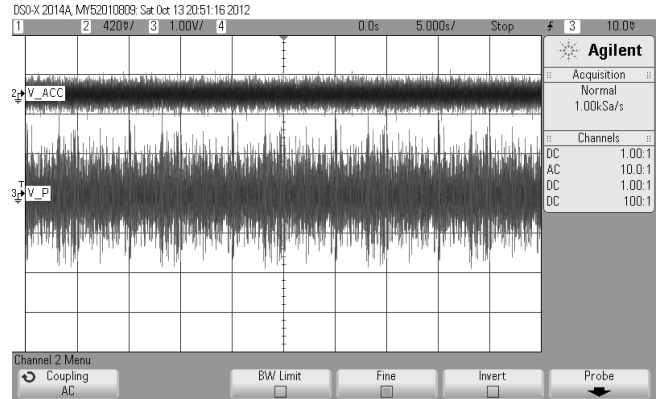


(b)

Fig. 2. Experimentally obtained waveforms of the open circuit output voltages under chirp excitation between 1-200Hz with a fixed amplitude input acceleration of 0.45g; input resistance of the scope -1MΩ: (a) rectangular beam (b) proposed beam.



(a)



(b)

Fig. 3. Time domain experimentally obtained waveforms of the output voltage, v_p , (lower trace) under random excitation at input acceleration of 0.145g (rms) and 74KΩ output load: (a) rectangular beam (b) proposed beam. The upper trace is the ADXL327 accelerometer output.

obtaining insight into the behavior of the system but is not sufficient for understanding how a real vibration energy harvesting device would behave when operated under broadband ambient vibration excitation. To this end, a filtered PSD (power spectral density) of a Gaussian white noise excitation signal with a 300Hz bandwidth was constructed in order to cover most of the sensitivity range of the generators. According to the experiment described in the previous sub-

The rms value of the input base acceleration amplitude was also extracted for the same time interval as:

$$a_{acc(rms)} = \sqrt{\frac{1}{50} \int_0^{50} a_{acc}^2 dt} \quad (4)$$

where a_{acc} and $a_{acc(rms)}$ are the instantaneous base acceleration (Fig. 3 upper traces) and the rms value of a_{acc} , respectively. Fig. 3 shows the random fluctuations of a_{acc} and v_p versus time.

The measurement was performed at a fixed base acceleration of 0.145g (rms) for each configuration and repeated for different resistive loads, R_L . For each configuration, three successive measurements were made to verify consistency. In each measurement the supporting beam was released and clamped again. Fig. 4 depicts the average power of the two configurations against load resistances. As can be seen, the trends of the results are indeed similar. In particular, the resultant maximum output power of the conventional rectangular beam (P_{conv1} , P_{conv2} , P_{conv3}) was found to be $\sim 4.6\mu\text{W}$ at an optimal load of $R_L=74\text{K}\Omega$. While the proposed system tends towards the same peak average power of $\sim 4.6\mu\text{W}$, it is achieved at a slightly lower optimal load (P_{cut1} , P_{cut2} , P_{cut3}). This

Fig. 5 depicts the normalized FFT spectrum of the random output voltage, v_p , time responses. It is evident that Fig. 5b shows three dominant voltage peaks, corresponding to the respective resonant modes arising from the three mechanical fingers.

Fig. 6 plots the statistical distribution of the proposed PZG output voltage, v_p , at an optimal load of $R_{L(opt)}=74\text{K}\Omega$ with applied accelerations of 0.145g (rms) and 0.24g (rms). It is evident that the distribution exhibits normal behavior, characterized by a standard deviation of $\sigma=0.5784\text{Vrms}$ and a zero mean, $\mu=0$, for the 0.145g (rms) case, while for an excitation of 0.24g (rms) we get $\sigma=0.9378\text{Vrms}$ and $\mu=0$. Hence, we confirm that the system responds linearly to a Gaussian random excitation input. This is probably due to the fact that the excitation level was set low enough to induce a small signal linear equilibrium condition in the system. Using the statistical parameter σ we can calculate the average

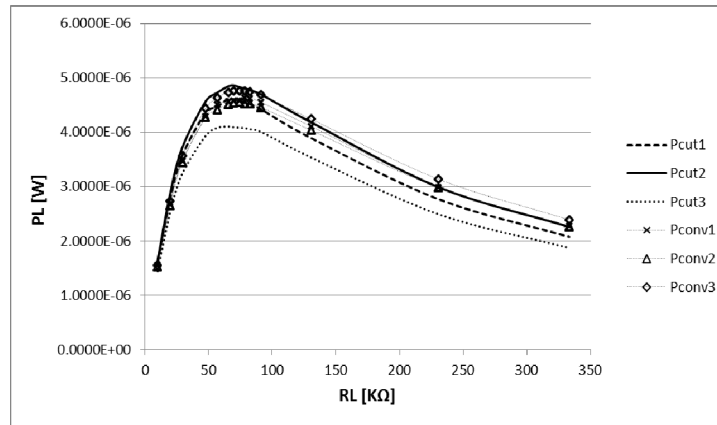


Fig. 4. Average output power vs. resistive load R_L for random excitation at a fixed input base acceleration of 0.145g (rms). P_{conv1} , P_{conv2} and P_{conv3} are the results of a three-measurement set carried out with the conventional configuration. P_{cut1} , P_{cut2} and P_{cut3} describe the three-measurement set results for the proposed generator. The experimental curves approach a maximum power point around $R_L=74\text{K}\Omega$.

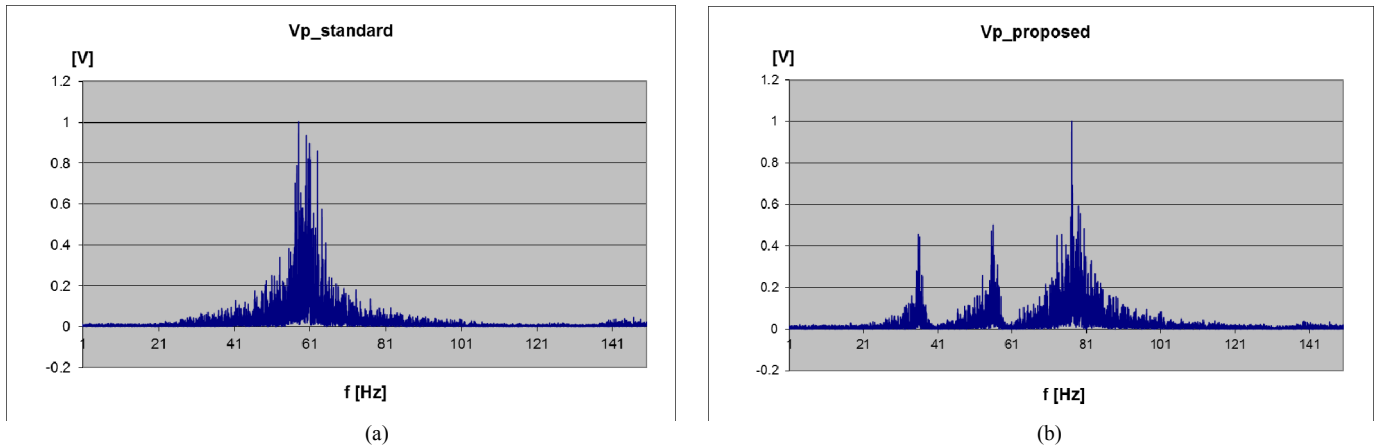


Fig. 5. Normalized FFT spectrum of the output voltage, v_p , under random excitation and with the same parameters as used in Fig. 3: (a) rectangular beam (b) proposed beam. Vertical units are volts [V] and horizontal units are Hertz [Hz].

can be explained by the fact that the dominant power exists between the 57Hz and the 76Hz frequencies (Fig. 2b), which is higher than the resonant frequency of the conventional structure. The systems were also tested under a higher acceleration of 0.24g (rms). In this case, the behavior of the systems was consistent with the previous setup and yielded the same optimal load, but with a peak output power of $\sim 12\mu\text{W}$.

output powers through,

$$P_L = \frac{\sigma^2}{R_{L(opt)}} \quad (5)$$

and we obtain $4.52\mu\text{W}$ and $11.88\mu\text{W}$, respectively. This, of course, matches the results obtained using the time domain

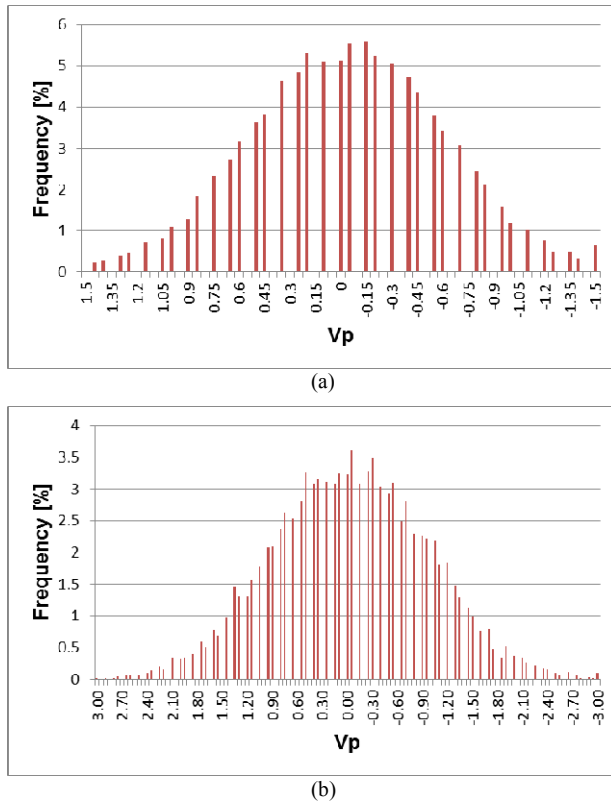


Fig. 6. Gaussian distribution of 50,000 time domain samples of the proposed generator output voltage, v_p , at an optimal load of $74\text{K}\Omega$. The standard deviation was found to be: (a) $\sigma=0.5784\text{Vrms}$ @ $a_{\text{acc(rms)}}=0.145\text{g rms}$, (b) $\sigma=0.9378\text{Vrms}$ @ $a_{\text{acc(rms)}}=0.24\text{g rms}$.

averaged power over a 50sec interval as calculated by (3).

IV. DISCUSSION AND CONCLUSIONS

In this paper, the bandwidth and the output power behavior of two PZG structures are assessed experimentally under weak wideband excitation. In the proposed method, the bandwidth is widened by attaching a shaped beam composed of three strips of increasing length. Each strip (finger) was chosen with a different length and, consequently, several frequency modes were obtained. The proposed structure does, indeed, widen the frequency band as seen in Fig. 2b. However, the magnitude of each mode is decreased compared with the results from the structure with a rectangular beam (Fig. 2a). In addition, it was also found that for the same beam area both systems exhibit similar peak and average output power under the same applied rms acceleration level (Fig. 4).

There are more ways to realize additional resonant modes [3]. This method, however, utilizes a given PZG platform and only the parameters of the attached beam are changed. It has been shown that the resultant frequency modes are discrete, in accordance with the number of employed strips. In order to achieve a higher number of overlapping frequency modes one

should carefully divide the beam into a higher number of narrow, equally spaced strips with appropriate proportions.

The harvesting concept is attractive because it is simple and cheap to construct and volume-effective. Specifically, the approach is valuable for shaping the frequency response of a commercial PZG before installing it into a time-varying environment. As previously mentioned, the average output power remained approximately the same as for the conventional PZG. Nevertheless, because in a realistic working environment the material properties of the PZG and the driving source tend to drift as a result of environmental changes such as temperature, the proposed solution can be utilized to broaden the bandwidth of the initial system by addressing the expected variations while continuing to provide useful output power.

It is challenging to process the low output levels associated with wideband vibrations using previously reported power converters [1], [2], [5], [8], [11], [12]. Future work will consider designing low-loss power conditioning circuits suitable for broadband weak excitations.

ACKNOWLEDGMENT

This research was supported by THE ISRAEL SCIENCE FOUNDATION (Grant No. 517/11).

REFERENCES

- [1] S. Roundy, P. K. Wright, and J. Rabaey, "A study of low level vibrations as a power source for wireless sensor nodes," *Comput. Commun.*, vol. 26, no. 11, pp. 1131–1144, July 2003.
- [2] I. C. Lien and Y. C. Shu, "Array of piezoelectric energy harvesting by the equivalent impedance approach," *Smart Materials and Structures*, vol. 21, no. 8, in press.
- [3] D. Zhu, M. J. Tudor and S. P. Beeby, "Strategies for increasing the operating frequency range of vibration energy harvesters: a review," *Meas. Sci. Technol.*, vol. 21, (2010) pp. 1-29.
- [4] H. Liu, et al., "Piezoelectric MEMS energy harvester for low-frequency vibrations with wideband operation range and steadily increased output power," *Journal of micromechanical systems*, vol. 20, no. 5, pp. 1131–1142, 2010.
- [5] C. Luo and H. F. Hofmann, "Wideband energy harvesting for resonant piezoelectric devices," in *Proc. IEEE Energy conversion congress and exposition (ECCE)*, USA, 2010, pp. 4171–4178.
- [6] Mide Technology Corporation, V20W piezoelectric vibration energy harvester, New-Vulture data sheet.
- [7] A. Shainkopf, G. Hadar and S. Ben-Yaakov, "Harvesting system for a piezoelectric generator", final project report in Hebrew 2011.
- [8] L. J. Blystad, E. Halvorsen and S. Husa, "Piezoelectric MEMS energy harvesting systems driven by harmonic and random vibrations," *IEEE Trans. Ultrason. Ferroelect., Freq. Control.*, vol. 57, no. 4, pp. 908–919, April 2011.
- [9] S. Mehraeen, S. Jagannathan and K. A. Corzine, "Energy harvesting from vibration with alternate scavenging circuitry and tapered cantilever beam," *IEEE Trans. Ind. Electron.*, vol. 57, no. 3, pp. 820-830, March 2010.
- [10] W. G. Li, S. He and S. Yu, "Improving power density of a cantilever piezoelectric power harvester through a curved L-shaped proof mass," *IEEE Trans. Ind. Electron.*, vol. 57, no. 3, pp. 868-876, March 2010.
- [11] N. Kriehly and S. Ben-Yaakov, "Piezoelectric harvesting circuit with extended input voltage range," in *Proc. IEEE 26 Convention of Electrical and Electronics Engineers in Israel (IEEEI)*, Eilat, Israel, 2010, pp. 670–674.
- [12] A. Tabesh and L. G. Frechette, "A Low-Power Stand-Alone Adaptive Circuit for Harvesting Energy From a Piezoelectric Micropower Generator," *IEEE Trans. Ind. Electron.*, vol. 57, no. 3, pp. 840-849, March 2010.